Eur. Phys. J. D (2014) 68: 269
DOI: 10.1140/epjd/e2014-50185-4

THE EUROPEAN
PHYSICAL JOURNAL D

Regular Article

Addressable parallel cavity-based quantum memory

Anton N. Vetlugin and Ivan V. Sokolov[a]

Faculty of Physics, St. Petersburg State University, Ul'janovskaya 3, 198504 Petrodvorets, St. Petersburg, Russia

Received 6 March 2014 / Received in final form 13 June 2014
Published online 25 September 2014 –

Abstract. We elaborate theoretically a model of addressable parallel cavity-based quantum memory for light able to store multiple transverse spatial modes of the input light signal of finite duration and, at the same time, a time sequence of the signals by side illumination. Having in mind possible applications for, e.g., quantum repeaters, we reveal the addressability of our memory, that is, its handiness for the read-out on demand of a given transverse quantized signal mode and of a given signal from the time sequence. The addressability is achieved by making use of different spatial configurations of pump wave during the write-in and the readout. We also demonstrate that for the signal durations of the order of few cavity decay times, better efficiency is achieved when one excites the cavity with zero light-matter coupling and finally performs fast excitation transfer from the intracavity field to the collective spin. On the other hand, the light-matter coupling control in time, based on dynamical impedance matching, allows to store and retrieve time restricted signals of the on-demand smooth time shape.

1 Introduction

Quantum memory for light is an essential part of quantum information protocols, such as quantum repeaters, distributed quantum computation, and quantum networks. A number of approaches based on storage in atomic ensembles and inhomogeneously broadened solid-state systems were developed recently (for reviews see [1–3]). The quantum non-demolition (QND) memory with the fidelity up to 70% was achieved [4] in cesium vapor. Recently there were reported the recall efficiencies of 69% for the optical gradient echo in praseodymium doped crystal [5] and of 87% with warm rubidium vapor [6].

A natural approach to the improvement of overall storage capacity is to develop multimode quantum memories. In particular, a possibility to store multiple temporal or spatial modes and to read-out one of the stored quantum signals in dependence on the outcome of an entangling Bell-type measurement performed at a remote station, promises a speed-up of quantum repeaters protocols by a factor, proportional to the number of stored modes [7].

Of particular interest might be the spatially multimode memories exploiting optical parallelism, where the number of stored modes is limited by diffraction or even by geometric aperture of atomic ensemble in some configurations. There were demonstrated theoretically the spatially-multimode QND quantum memory for images [8] and the spatially resolving off-resonant Raman-type memory [9]. The quantum volume hologram of references [10,11] combines the Raman-type interaction with non-collinear configuration of the interacting waves similar to classical volume hologram. The memories based on the on-resonant interaction in Λ-schemes were extended to spatially-multimode case for the fast and adiabatic [12,13] modes of operation. An extensive numerical 3D analysis [14] of parallel Λ-type memory capacity, performed in the paraxial approximation for a realistic (cylindrical) shape of atomic ensemble, has revealed a universal role of the cell optical depth and of the Fresnel number F for a wide range of these parameters. Storage and retrieval of a set of transverse modes in the orbital angular momentum domain was demonstrated experimentally [15].

In this paper we elaborate a model of addressable parallel cavity-based quantum memory for light.

The use of optical cavity allows for smaller optical depth of storage medium [16,17] and makes it possible to control the memory parameters through modulation of the atom-cavity coupling or detuning [18,19] We consider a high-quality ring single-port cavity with a large number of transverse cavity modes and with an ensemble of motionless atoms with long-lived ground state spin levels, confined inside the cavity.

Having in mind possible applications for, e.g., quantum repeaters, we concentrate on the addressability of our memory, that is, on its handiness for the read-out "on demand" of a given quantized signal mode specified by its transverse index and position in time. For storage medium we use the configuration of quantum volume hologram of [10,11], extended to the case of tunable propagation direction of classical control field in order to provide the on demand read-out.

The use of multi-atomic ensemble which occupies a significant part of the cavity volume, as opposed to variety of

[a] e-mail: sokolov.i.v@gmail.com

single-atom microcavity-based memories, makes it possible to achieve storage in multiple spatial modes of the collective spin and provides sensitivity to the control field propagation direction. In particular, by using non-collinear signal and pump waves with time-dependent relative propagation angle one can store and retrieve temporal shape of the signal with some analogy to the controlled reversible inhomogeneous broadening (CRIB) based memories, as discussed in detail in reference [20].

In what follows we reveal two spatial configurations both allowing for 2D addressability of the memory. We demonstrate that for the geometries close to the co- and counter-propagating illumination by the pump wave, one can retrieve into a high-quality output port any of stored signal mode specified by its 2D transverse index. In case of side illumination, the on-demand retrieval of the mode specified by one component of transverse index and by its position in time sequence is possible.

Another issue we address here is the optimal shaping of the pump and the signal pulses in time. Since the storage of the relatively short input signals might be of interest in order to achieve better memory capacity, we do not apply here the "bad cavity" limit and examine storage of spatially multimode signals of given finite duration comparable with the cavity decay time.

In order to effectively excite a high-quality cavity with active medium inside, one has to minimize reflection of the input signal during the write-in. This can be achieved by the impedance matching, which implies matching of the absorption by medium, placed inside the cavity, with the cavity losses. This approach works perfectly in the bad cavity limit for the spin, the atomic frequency comb (AFC) [21], and the CRIB [22] memories. Another approach is provided by the time-reversal operation [17,18], developed in the theory of linear filtering [23], where the input signal is time-reversed with respect to the pulse emitted from the memory. In both methods a problem of optimal time shape of the light-matter coupling arises.

We demonstrate that in the impedance matching approach one can find the time shape of the coupling (actually of the pump field) such that the effectively stored signal has smooth form, suited for possible applications, for transverse modes within the diffraction limited angle. On the other hand, the optimal write-in efficiency for given signal duration is achieved by the time-reversal excitation for the coupling temporarily off ("empty" cavity), followed by fast excitation transfer from the quantized intracavity field to the collective spin. In the bad cavity limit the reflection losses are eliminated in both modes of the memory operation.

The paper is organized as follows. In Section 2 we introduce our parallel quantum memory scheme in cavity configuration and demonstrate 2D transverse addressability of the scheme for the co- and counter-propagating, with respect to quantized signal, pump wave. In Section 3 we consider memory configuration, where the classical pump field illuminates the memory cell from orthogonal side direction, as shown in Figure 2. The 1D transverse addressability and the 1D addressability in time domain (that is, the possibility to retrieve on demand of a signal from time sequence) are demonstrated.

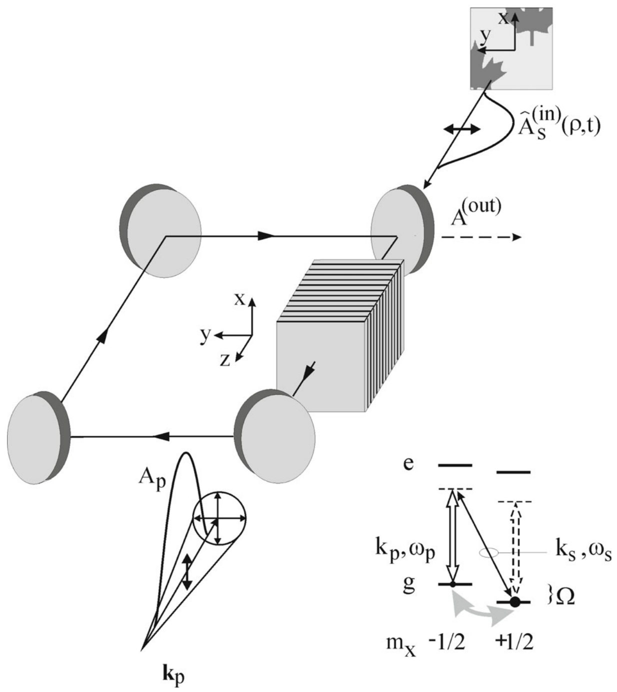

Fig. 1. Schematic of addressable cavity based parallel quantum memory for the counter-propagating illumination.

The write-in efficiency for time-reversal approach in dependence on transverse momentum of the input signal spatial modes is analyzed in Section 4. A comparison with the impedance matching method is given. In Section 5 we come to conclusion. In Appendix A we briefly outline the effect of finite transverse size of the intracavity field patterns, and in Appendix B we relate the problem of optimal efficiency of our memory to the dynamics of the excitations number by the time-reversed evolution, and argue in favor of time-reversal optimization for the specific mode of light-matter coupling control, described above.

2 Memory scheme and 2D addressability

The scheme of the memory is shown in Figure 1.

The spatially multimode input signal is stored in a spatially distributed ensemble of motionless atoms. The storage medium is placed inside a high-quality single-port ring cavity. The atoms with angular momentum of $J = 1/2$ both in the ground and in the excited states are located at random positions. The long-lived ground state spin of an atom $\boldsymbol{J}^a$ is initially oriented along the constant magnetic field in the vertical direction x. The atomic spins rotate around the vertical axis with a circular frequency Ω.

The input signal wave, carrying an optical image or 2D data set, is a weak quantized y-polarized off-resonant field at frequency ω_s entering the cavity in $+z$ direction. This spatially multimode input field with the slowly varying amplitude $A^{(in)}(\boldsymbol{\rho}, t)$ at the input cavity port, where

$\boldsymbol{\rho} = \{x, y\}$ – transverse coordinate, is considered in the paraxial approximation.

In this Section we consider the co- and counter-propagating geometry, where classical off-resonant x-polarized plane pump wave at frequency ω_p with the slow amplitude $A_p(t)$, assumed to be real, is allowed to illuminate the medium in a direction close to z or $-z$, similar to quantum volume hologram of [10]. The Raman resonance condition for the memory is $\omega_s = \omega_p + \Omega$, and for the light-matter entanglement is $\omega_s = \omega_p - \Omega$. We assume here the entanglement frequency band to be out of resonance with the cavity frequency ω_c.

We start from the quantum non-demolition (QND) light-matter interaction which leads [1] to the following basic effects: (i) the Faraday rotation of light polarization due to longitudinal quantum z-component of collective atomic spin in a given location; and (ii) the atomic spin rotation, caused by the unequal light shifts of the ground state sub-levels with $m_z = \pm 1/2$ in the presence of quantum fluctuations of circular light polarizations. Note that for the time-dependent pump field the light shifts induced by classical field itself are compensated in the $J = 1/2 \leftrightarrow J = 1/2$ levels scheme. The relevant part of the Hamiltonian is

$$H = \frac{2\pi\omega_s |d|^2}{(\omega_{eg} - \omega_s)L} \int_V d\boldsymbol{r} \sum_a J_z^a(t) S_z(\boldsymbol{r}, t)\delta(\boldsymbol{r} - \boldsymbol{r}_a). \quad (1)$$

Here ω_{eg} is the frequency of atomic transition, L is the ring cavity length, d is the dipole matrix element, J_z^a and S_z are z-projections of the ground state atomic spin and the Stokes vector. For the intracavity quantized field, which is assumed to be spatially multimode in transverse direction but corresponds to a single longitudinal mode, we use the commutation relation

$$[A(\boldsymbol{\rho}, t), A^\dagger(\boldsymbol{\rho}', t)] = \delta(\boldsymbol{\rho} - \boldsymbol{\rho}'), \quad (2)$$

where $A^\dagger A$ gives the photon number per cm^2 of the cavity cross-section. For the pump field amplitude we use the same units, and for the input signal field the commutation relation reads,

$$[A^{(in)}(\boldsymbol{\rho}, t), A^{(in)\dagger}(\boldsymbol{\rho}', t')] = \delta(\boldsymbol{\rho} - \boldsymbol{\rho}')\delta(t - t'), \quad (3)$$

where $A^{(in)\dagger} A^{(in)}$ is the input photon number per cm^2 s.

In order to make possible the addressable read-out of the memory, we consider the pump wave propagation direction slightly different from z or $-z$. We introduce the transverse pump wave momentum $\boldsymbol{q}_p$ in the $\{x, y\}$ plane, where $q_p/k_p \ll 1$, and assume $\boldsymbol{k}_p = \{q_{px}, q_{py}, f_g k_{p\|}\}$. Here f_g is the geometric factor, $f_g = \pm 1$ for the pump wave propagating close to $\pm z$ direction. The cavity field amplitude is:

$$A_p(t) \exp\{i(f_g k_{p\|} z + \boldsymbol{q}_p \boldsymbol{\rho} - \omega_p t)\}\mathbf{e}_x + A(\boldsymbol{\rho}, t) \exp\{i(k_s z - \omega_s t\}\mathbf{e}_y, \quad (4)$$

where $A(\boldsymbol{\rho}, t)$ is the weak quantized signal field. The Stokes vector z-component oscillates in time at frequency Ω due to beatings between the pump and the signal wave,

$$S_z^{(c)}(z, \boldsymbol{\rho}, t) = 2A_p(t)\mathrm{Im}[A(\boldsymbol{\rho}, t) \times \exp\{i[(k_s - f_g k_{p\|})z - \boldsymbol{q}_p\boldsymbol{\rho} - \Omega t]\}]. \quad (5)$$

The density of the ground state collective spin is $\boldsymbol{J}(\boldsymbol{r}) = \sum_a \boldsymbol{J}^a \delta(\boldsymbol{r} - \boldsymbol{r}_a)$. The averaged over random positions of the atoms commutation relation for the y, z components of the collective spin is

$$\overline{[J_y(\boldsymbol{r}), J_z(\boldsymbol{r}')]} = i \sum_a \langle J_x^a \rangle \overline{\delta(\boldsymbol{r} - \boldsymbol{r}_a)\delta(\boldsymbol{r}' - \boldsymbol{r}_a)}^a = i n_a \langle J_x^a \rangle \delta(\boldsymbol{r} - \boldsymbol{r}'). \quad (6)$$

Here n_a is the average density of atoms. The field-like variable for the spin subsystem,

$$B(\boldsymbol{r}, t) = \{J_y(\boldsymbol{r}, t) + iJ_z(\boldsymbol{r}, t)\}/\sqrt{2n_a\langle J_x^a \rangle},$$

obeys the standard boson commutation relation:

$$\overline{[B(\boldsymbol{r}, t), B^\dagger(\boldsymbol{r}', t)]} = \delta(\boldsymbol{r} - \boldsymbol{r}'). \quad (7)$$

In view of the fact that the atoms are prepared in the spin up state, the operator $B^\dagger$ can be considered as the creation operator for atoms in the spin down state.

The evolution of our memory is described by the standard "in-out" relations for optical cavity taking into account diffraction, the effective QND interaction (1), and the interaction of collective atomic spin with constant magnetic field described by the Hamiltonian density $\hbar\Omega B^\dagger(\boldsymbol{r}, t)B(\boldsymbol{r}, t)$. Using in the Heisenberg picture the commutation relations (2) and (7), we arrive at the following equations for the field and atomic variables,

$$\frac{\partial A(\boldsymbol{\rho}, t)}{\partial t} = \left[i\left(\omega_s - \omega_c + \frac{c}{2k_c}\nabla_\perp^2\right) - \frac{C}{2}\right] A(\boldsymbol{\rho}, t) + \sqrt{C}A^{(in)}(\boldsymbol{\rho}, t) - i\tilde{k}(t) \times \int_L dz \Big([B(z, \boldsymbol{\rho}, t) - h.c.] \times \exp\{i[-(k_s - f_g k_{p\|})z + \boldsymbol{q}_p\boldsymbol{\rho} + \Omega t]\}\Big), \quad (8)$$

$$\frac{\partial B(z, \boldsymbol{\rho}, t)}{\partial t} = -i\Omega B(z, \boldsymbol{\rho}, t) - i\tilde{k}(t) \times [A(\boldsymbol{\rho}, t) \exp\{i[(k_s - f_g k_{p\|})z - \boldsymbol{q}_p\boldsymbol{\rho} - \Omega t]\} - h.c.]. \quad (9)$$

Here ω_c is the cavity frequency, C – cavity decay rate, the light-matter coupling parameter is given by:

$$\tilde{k}(t) = \frac{\pi\omega_s |d|^2}{\hbar(\omega_{eg} - \omega_s)L}\sqrt{2n_a\langle J_x^a \rangle} A_p(t). \quad (10)$$

We consider the amplitude $A(\boldsymbol{\rho}, t)$ as slow in the frame rotating at $\omega_s = \omega_p + \Omega$ and constant along z, thus excluding the entanglement frequency sideband. This is consistent with the equations above if one introduces the slow in time and constant along z collective spin amplitude $B(\boldsymbol{\rho}, t)$,

$$B(z,\boldsymbol{\rho},t) = \frac{1}{\sqrt{L_z}} B(\boldsymbol{\rho},t)\exp\{i[(k_s - f_g k_{p\|})z - \Omega t]\} + \ldots, \tag{11}$$

$$B(\boldsymbol{\rho},t) = \frac{1}{\sqrt{L_z}}\int_{L_z} dz B(z,\boldsymbol{\rho},t) \times \exp\{-i[(k_s - f_g k_{p\|})z - \Omega t]\}. \tag{12}$$

Here "..." stands for the contribution of other longitudinal modes needed for consistency with (7), L_z is the atomic ensemble length in z-direction. We assume that the pump wave propagation angle is small, when $(k_p - k_{p\|})L_z \ll 2\pi$, and substitute $k_{p\|} \to k_p$ in (12). Since $k_{p\|} \approx k_p\left(1 - q_p^2/2k_p^2\right)$, this implies $q_p \ll \sqrt{2\pi k_p/L_z}$. Hence, the amplitude $B(\boldsymbol{\rho}, t)$ does not implicitly depend on q_p and one can apply the definition above when the pump wave transverse momentum $\boldsymbol{q}_p$ is different for the write-in and the readout stages. The commutation relation for this amplitude,

$$[B(\boldsymbol{\rho},t), B^\dagger(\boldsymbol{\rho}',t)] = \delta(\boldsymbol{\rho} - \boldsymbol{\rho}'), \tag{13}$$

is similar to that of the intracavity quantized field (2), and $B^\dagger(\boldsymbol{\rho},t)B(\boldsymbol{\rho},t)$ corresponds to the number of flipped spins per cm^2 of the cavity cross section.

Next, we substitute (12) into the evolution equations, retain only the slow in time (on the scale $1/\Omega$) and in the longitudinal direction z (on the scale $\lambda_s = 2\pi/k_s$) contributions, and go over to the Fourier domain in transverse dimension by introducing the amplitudes

$$a(\boldsymbol{q},t) = \int d\boldsymbol{\rho}\, A(\boldsymbol{\rho},t)e^{-i\boldsymbol{q}\cdot\boldsymbol{\rho}},$$

and similar for $b(\boldsymbol{q}, t)$ and $a^{(in)}(\boldsymbol{q}, t)$. We arrive at the evolution equations of the form

$$\frac{\partial a(\boldsymbol{q},t)}{\partial t} = \left[i\left(\omega_s - \omega_c - \frac{q^2 c}{2k_c}\right) - \frac{C}{2}\right]a(\boldsymbol{q},t) - ik(t)b(\boldsymbol{q}-\boldsymbol{q}_p,t) + \sqrt{C}a^{(in)}(0,\boldsymbol{q},t), \tag{14}$$

$$\frac{\partial b(\boldsymbol{q}-\boldsymbol{q}_p,t)}{\partial t} = -ik(t)a(\boldsymbol{q},t). \tag{15}$$

The coupling constant

$$k(t) = \tilde{k}(t)\sqrt{L_z}, \tag{16}$$

gives the frequency of state exchange between the cavity fields $A(\boldsymbol{\rho}, t)$ and $B(\boldsymbol{\rho}, t)$. For both geometries, $f_g = \pm 1$, the evolution equations and the coupling constant look similar, but the signal wave is coupled to different degrees of freedom of the collective spin.

The equations above apply both to the write-in and the readout stages of the memory and demonstrate the transverse 2D addressability of our scheme. By choosing the transverse momentum $\boldsymbol{q}_p$ (i.e. the propagation angle)

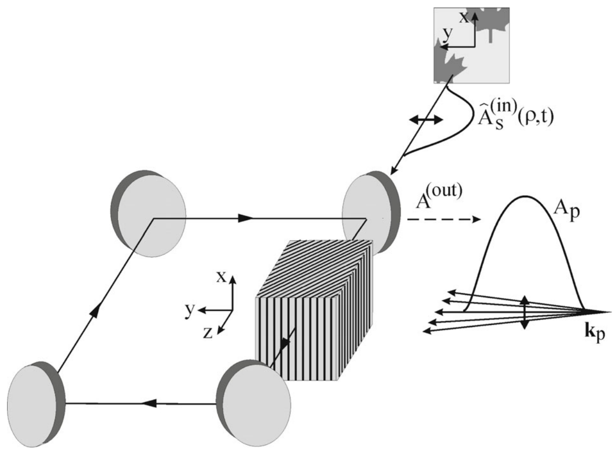

Fig. 2. Addressability in time domain by the side illumination.

of the pump wave, one couples the intracavity quantized field amplitude $a(\boldsymbol{q}, t)$ with the collective spin amplitude $b(\boldsymbol{q} - \boldsymbol{q}_p, t)$, as seen from equations (14) and (15). This makes it possible to readout in a given direction within the angle range supported by the cavity (see Sect. 4) any transverse spatial mode of the collective spin during the retrieval stage of the memory.

In this consideration we have exploited the basis of plain waves with single transverse momentum. This is common approximation in the limit of wide-aperture systems. In Appendix A we present some estimates for more realistic configuration with a wide-aperture near-planar cavity and finite transverse size of the intracavity field patterns.

The multivariate nature of the memory together with the addressability makes it advantageous for use in quantum repeaters. One can store in the memory multiple transverse modes and wait for the outcome of parallel entangling Bell-type measurement, performed at a remote station. In case of success, the relevant transverse collective spin mode is retrieved into a high quality output channel with the use of the Fourier processor or another device. This promises a speed-up of quantum repeater protocol by a factor proportional to the number of stored modes [7].

3 Memory addressability by side illumination

Similar to classical volume hologram, our memory allows to write and retrieve the signal wavefronts by illuminating the memory cell with the pump wave propagating at arbitrary relative angle. It was shown [20] that by using non-collinear signal and pump waves with the time-dependent relative propagation angle one can reproduce by retrieval the temporal shape of the signal with some analogy to CRIB based memories.

In this section we extend our model to the close to orthogonal side illumination in $+y$ direction, as shown in Figure 2, and demonstrate its 2D addressability in space-time domain for the short time restricted signal pulses.

Similar to Section 2, the x-polarized classical pump wave is allowed to have small transverse momentum $\boldsymbol{k}_{p\perp}$ in $\{x, z\}$ plane, where $k_{p\perp} \ll k_p$, and $\boldsymbol{k}_p = \{k_{px}, k_{p\|}, k_{pz}\}$. The expressions for the cavity field amplitude and the Stokes vector z-projection, substituting (4) and (5), are

$$A_p(t)\exp\{i(k_{p\|}y + k_{px}x + k_{pz}z - \omega_p t)\}\mathbf{e}_x + A(\boldsymbol{\rho}, t)\exp\{i(k_s z - \omega_s t)\}\mathbf{e}_y, \quad (17)$$

$$S_z^{(s)}(z, \boldsymbol{\rho}, t) = 2A_p(t)\mathrm{Im}[A(\boldsymbol{\rho}, t) \times \exp\{i(k_s z - k_{p\|}y - k_{px}x - k_{pz}z - \Omega t]\}]. \quad (18)$$

The memory evolution equations are derived in the same steps as in Section 2 by using the QND Hamiltonian and the commutation relations. The only distinction from equations (8) and (9) is due to the spatial modulation factors. Assume for k_{pz} one of the values $k_{pz}^{(n)} = 2\pi n/L_z$, where $n = 0, \pm 1, \ldots$ The slow in $\{x, y\}$ plane and in time collective spin amplitude $B_n(\boldsymbol{\rho}, t)$ is now related to the local amplitude $B(z, \boldsymbol{\rho}, t)$ as follows,

$$B(z, \boldsymbol{\rho}, t) = \frac{1}{\sqrt{L_z}} B_n(\boldsymbol{\rho}, t) \times \exp\{i[(k_s - k_{pz}^{(n)})z - k_{p\|}y - \Omega t]\} + \ldots, \quad (19)$$

$$B_n(\boldsymbol{\rho}, t) = \frac{1}{\sqrt{L_z}} \int_{L_z} dz B(z, \boldsymbol{\rho}, t) \times \exp\{-i[(k_s - k_{pz}^{(n)})z - k_{p\|}y - \Omega t]\}. \quad (20)$$

It is evident from (19) that the interference pattern generated in the medium is now oriented as shown in Figure 2, and at the readout stage the quantized field can be viewed to as produced by the pump wave scattering on this spatial structure.

For small enough deviations of the pump propagation direction from perpendicular to $\{x, z\}$ plane, we assume $|k_p - k_{p\|}|L_y \ll 2\pi$ and substitute in the equations above $k_{p\|} \to k_p$. Since $k_{p\|} \approx k_p(1 - k_{p\perp}^2/2k_p^2)$, this implies $k_{p\perp} \ll \sqrt{2\pi k_p/L_y}$. Similar to Section 2, the amplitude $B_n(\boldsymbol{\rho}, t)$ does not implicitly depend on k_{px} and one can apply the definition above when the pump wave transverse momentum k_{px} is different for the write-in and the readout stages. Moreover, the collective spin spatial modes specified by (20) for different pump wave directions in $\{y, z\}$ plane (that is, different n's) are orthogonal, and we arrive at the commutation relation

$$[B_n(\boldsymbol{\rho}, t), B_m^\dagger(\boldsymbol{\rho}', t)] = \delta(\boldsymbol{\rho} - \boldsymbol{\rho}')\delta_{nm}. \quad (21)$$

Following the same steps as in Section 2, we obtain the memory evolution equations, valid for both the write-in and retrieval, similar to (14) and (15), where one substitutes $b(\boldsymbol{q} - \boldsymbol{q}_p, t) \to b_n(\boldsymbol{q} - \boldsymbol{e}_x k_{px}, t)$, with the same coupling constant.

In space domain the memory demonstrates the 1D addressability: by changing from the write-in to the retrieval stage the pump wave propagation direction in (x, y) plane, one can on demand change the q_x component of the retrieved signal transverse momentum.

Since for given $k_{pz}^{(n)}$ the light-matter coupling involves one of the independent longitudinal modes of the collective spin, the memory is able to store at the same time many signals from a time sequence, given each signal was written with proper pump wave direction in the $\{y, z\}$ plane. For the retrieval on demand of a given stored signal from the sequence, the pump wave of the relevant propagation direction is used. The number of addressable longitudinal modes of the matter is limited by the condition $k_{p\perp} \ll \sqrt{2\pi k_p/L_y}$, where $k_{pz}^{(n)} = 2\pi n/L_z$, and is estimated as $2|n| \ll 2L_z/\sqrt{\lambda_p L_y}$.

4 Write-in efficiency and capacity

Given one neglects the atomic relaxation, the deteriorative effect on efficiency in the cavity-based memory is due to the signal field reflection from the input mirror. For the slow as compared to the cavity decay time $\sim 1/C$ signals the memory operation is typically considered in the bad cavity limit, where one can suppress the reflection by using the cavity impedance matching. For the time restricted signals two basic approaches were elaborated: (i) the time reversal method, where temporal profile of the input signal is taken as the inverted in time decay pattern of the memory; and (ii) the approach based on the control of the interaction parameters which provide minimal reflection for a given temporal shape of the input signal (one could call the last one a dynamical impedance matching).

In Appendix B we present a reasoning which shows that for the given signal duration T the optimal efficiency is achieved by the time reversed input signal given the following mode of the memory operation is used: the light-matter coupling is temporarily switched off, and after the cavity is excited by the signal, the coupling is applied in the form of a short π-pulse, which swaps the intracavity signal to the collective spin. In what follows we examine the memory efficiency in dependence of the signal duration and of the transverse mode index $\boldsymbol{q}$ for this mode of operation, and bear comparison with the efficiency for the time-restricted smooth signal found in the impedance matching approach.

A natural measure for time intervals is in units of the cavity decay time $1/C$. Let us introduce dimensionless variables $Ct = \tau$, $CT = \mathcal{T}$, $(\omega_c - \omega_s)/C = \Delta$, $\tilde{\Delta}(q) = \Delta + q^2/q_c^2$, where $q_c^2 = 2k_c C/c$, and q_c is the spatial bandwidth of the cavity due to diffraction. We denote the intracavity amplitudes as:

$$a(\boldsymbol{q}, t) = \alpha(\boldsymbol{q}, \tau), \qquad b(\boldsymbol{q}, t) = \beta(\boldsymbol{q}, \tau),$$

and introduce the free space "in" ("out") amplitudes

$$a^{(in)}(0, \boldsymbol{\rho}, t)/\sqrt{C} = \alpha^{(in)}(0, \boldsymbol{\rho}, \tau),$$

such that $\alpha^{(in)\dagger}\alpha^{(in)}$ is the density of quanta per cm^2 per unit time,

$$\left[\alpha^{(in)}(0, \boldsymbol{\rho}, \tau), \alpha^{(in)\dagger}(0, \boldsymbol{\rho}', \tau')\right] = \delta(\boldsymbol{\rho} - \boldsymbol{\rho}')\delta(\tau - \tau'). \quad (22)$$

The evolution equations, including that for the outgoing field, are:

$$\begin{aligned}\frac{\partial\alpha(\boldsymbol{q},\tau)}{\partial\tau} &= -\left[i\tilde{\Delta}(q)+\frac{1}{2}\right]\alpha(\boldsymbol{q},\tau)\\ &\quad - i\kappa(\tau)\beta(\boldsymbol{q},\tau)+\alpha^{(in)}(0,\boldsymbol{q},\tau),\\ \frac{\partial}{\partial\tau}\beta(\boldsymbol{q},\tau) &= -i\kappa(\tau)\alpha(\boldsymbol{q},\tau),\\ \alpha^{(out)}(0,\boldsymbol{q},\tau) &= -\alpha^{(in)}(0,\boldsymbol{q},\tau)+\alpha(\boldsymbol{q},\tau). \end{aligned} \tag{23}$$

The dimensionless coupling parameter is $\kappa(\tau) = k(t)/C$, small transverse momentum of the pump wave is set to zero for simplicity. Assume the incoming signal of duration $\mathcal{T}$ to be classical field of the time reversed exponential shape,

$$\alpha^{(in)}(\boldsymbol{q},\tau) = \begin{cases} \alpha^{(in)}(\boldsymbol{q},0)e^{\tau/2} & \mathcal{T}\geq\tau\geq 0,\\ 0 & 0>\tau, \quad \tau>\mathcal{T}. \end{cases} \tag{24}$$

The cavity field evolution equation (23) for the "coupling off" stage, $\kappa = 0$, is easily solved. We define the efficiency $\eta(\boldsymbol{q})$ for a given transverse index $\boldsymbol{q}$ as the ratio of energy stored by the time $\mathcal{T}$ in the cavity mode $\boldsymbol{q}$ to the energy of incoming signal for the same $\boldsymbol{q}$. After simple calculation we arrive at

$$\eta(\boldsymbol{q}) = \frac{1}{1+\tilde{\Delta}^2(\boldsymbol{q})}\left(1-e^{-\mathcal{T}}+2\frac{1-\cos\left(\tilde{\Delta}(\boldsymbol{q})\mathcal{T}\right)}{e^{\mathcal{T}}-1}\right). \tag{25}$$

Provided the state transfer at $\tau\to\mathcal{T}$ to the collective spin is performed by modulation of the coupling parameter $\kappa(\tau)$ in form of a short π-pulse of duration Δt, where $L/c \ll \Delta t \ll 1/C$, we consider the result (25) as the write-in efficiency of the memory. The condition $\Delta t \ll 1/C$ implies that the transverse signal field modes within the cavity bandwidth are effectively transferred, and the off-resonant longitudinal modes are not involved for Δt much exceeding the round-trip time L/c.

The efficiency dependence of the time reversed signal duration (in units of the cavity decay time) and of the effective mismatch of inclined waves $\tilde{\Delta}\to q^2/q_c^2$ for $\omega_c = \omega_s$, is shown in Figure 3. For large enough signal duration, $\mathcal{T}\geq 1$, the transverse modes with $q\leq q_c$ are written with the efficiency exceeding 0.5. For the beamsplitter type memories this is sufficient for the storage preserving positive coherent information of [24,25]. The resolving power in space of our memory is characterized by the transverse size $d\sim 2\pi/q_c\sim 2\pi\sqrt{c/C2k_c}$ of an input image element which can be effectively stored. Since $c/C = L_{eff}$ is the length passed by light inside the cavity during the decay time, the estimated size d and the number $N = S_\perp/d^2$ of stored transverse modes, where $S_\perp$ is the transverse cross-section of atomic ensemble, are limited by diffraction at this effective length. The plot Figure 3 also demonstrates that good multimode efficiencies are available for the signal duration of the order of few cavity decay times, and it is possible to operate the memory outside the bad cavity limit $\mathcal{T}\to\infty$.

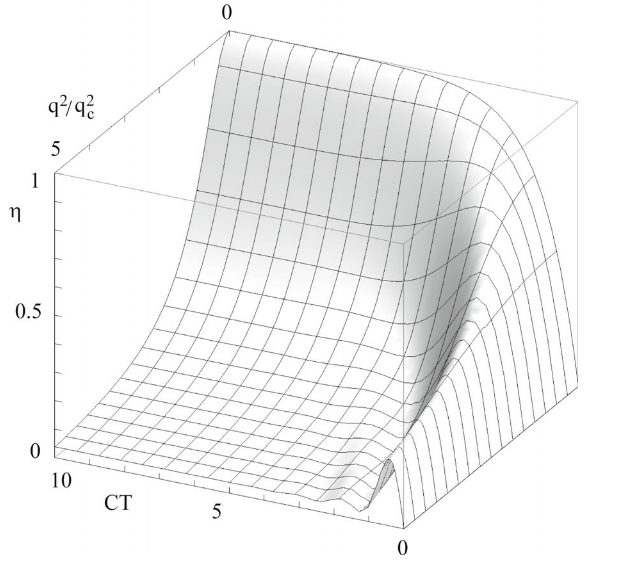

Fig. 3. Write-in efficiency $\eta(\boldsymbol{q})$ by the optimal time-reversal operation. Here $q^2/q_c^2 = \tilde{\Delta}$ is the propagation angle dependent frequency mismatch, $C T = \mathcal{T}$ – normalized signal duration.

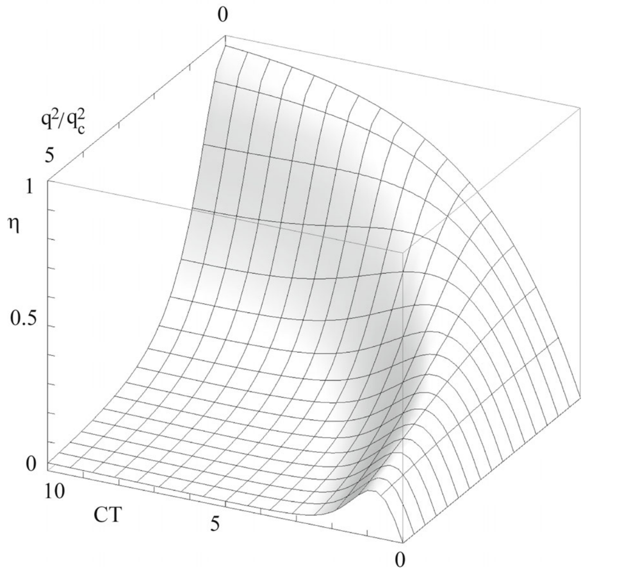

Fig. 4. Write-in efficiency by the impedance matching operation.

For comparison we plot in Figure 4 write-in efficiency for the time-restricted smooth symmetrical input signal of the form $\sim\sin(\pi\tau/\mathcal{T})$. Storage and retrieval of spatially multimode signals of the on-demand time shape for similar parallel memory configuration was considered [26] in the impedance matching approach, extending that of [27] onto the multiatomic storage medium. In reference [26] the time shape of the coupling parameter $\kappa(t)$ is estimated which matches the input signal (see Fig. 5). In agreement with the consideration given in Appendix, the memory operation with the time-reversal excitation of "empty" cavity followed by fast excitation transfer to the collective spin is more efficient, but does not allow for the control of the signal shape.

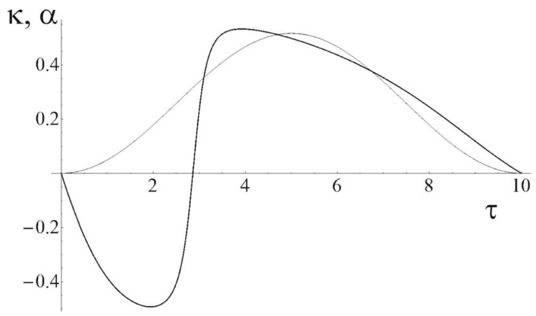

Fig. 5. Time shape of the coupling parameter $\kappa(\tau)$ (bold line) which matches the input signal $\sim\sin(\pi\tau/\mathcal{T})$ (thin line) for $\mathcal{T}$ = 10, arb. units

5 Conclusion

We have elaborated theoretically a model of parallel cavity-based quantum memory for light, able to store multiple transverse spatial modes of the input light signal of finite duration. Having in mind possible applications for, e.g., quantum repeaters, we have revealed the addressability of our memory, that is, its handiness for the read-out on demand of a given transverse quantized signal mode and, in one of configurations, of a given signal from time sequence. The addressability is achieved by making use of different spatial configurations of the pump wave during the write-in and the readout. We have estimated the memory capacity in terms of the number of efficiently stored transverse and temporal modes. For transverse modes the capacity is limited by diffraction at the propagation length within the cavity lifetime.

We have compared methods of the memory control for time restricted input signals. For the signal durations of the order of few cavity decay times, better efficiency is achieved when one excites the cavity with zero light-matter coupling and finally performs fast excitation transfer from the intracavity field to the collective spin. On the other hand, the light-matter coupling control in time, based on impedance matching, allows to store and retrieve time restricted signals of the on-demand smooth time shape.

This research was supported by the Russian Foundation for Basic Research under the projects 12-02-00181a and 13-02-00254a. The authors acknowledge Saint-Petersburg State University for research Grant 11.38.70.2012, and the support from the EU-Russia program ERA.Net Rus under the NANOQUINT project.

Appendix A

In this Appendix we briefly outline the effect of finite transverse size of the intracavity field patterns in our cavity-based memory.

The basis of single transverse momentum waves we exploit in this work is widely used as a common approximation in the theory of spatial phenomena in wide-aperture cavity-based systems, such as nonlinear transverse patterns (transverse optical solitons, domain walls etc.) and quantum imaging [28,29]. In our paper we address just this limit: a wide-aperture cavity with high transverse mode degeneracy.

As known ([30], Chap. 16), transverse multimode cavity in Gaussian approximation has equally spaced in frequency domain eigenmodes of the HG (Hermite-Gaussian) profile in both transverse directions. Consider for simplicity a wide aperture near-planar linear cavity of length L with the mirrors of radius $R \gg L$. The essential parameters are the waist radius w, where $kw^2 = \sqrt{RL}$, and frequency spacing $\Delta\omega_{HG} = c/\sqrt{RL}$ (here k is the wave number). A transverse field profile, constructed as a superposition of the HG modes, demonstrates oscillatory evolution in both transverse directions at frequency $\Delta\omega_{HG}$.

As a more realistic pattern, close to single transverse momentum wave of our paper, one can consider the product of corresponding plane wave profile and Gaussian envelope of waist w. Though such a pattern is not the cavity transverse eigenmode, it can be represented as a coherent state-like superposition of the HG modes of the relevant transverse coordinate. As we shall discuss elsewhere, the analogy with the coherent state-like packets of the HG profiles allows one to estimate the variance $\langle\Delta n^2\rangle$ of the index n of the HG eigenmodes that compose the pattern with given average $\langle n\rangle$ via

$$\sqrt{\langle\Delta n^2\rangle} \sim \sqrt{\langle n\rangle}.$$

That is, mean energy of the pattern in frequency units is $\langle n\rangle\Delta\omega_{HG}$, while its frequency width is $\sqrt{\langle n\rangle}\Delta\omega_{HG}$. A near-resonant signal field effectively excites patterns within the cavity linewidth, $\langle n\rangle \sim C/\Delta\omega_{HG}$. One can achieve the regime of many transverse modes, $\langle n\rangle \gg 1$, by using the mirrors of large enough radius with $\Delta\omega_{HG} \ll C$.

In the regime of many transverse modes we consider here, the frequency width $\sqrt{\langle n\rangle}\Delta\omega_{HG}$ of the introduced above quasi-plane modes is small as compared to C. Hence, the frequency width can be neglected if the cavity is excited with the time-restricted signal of duration $T \geq 1/C$, when one can consider transverse plane waves modulated with Gaussian envelope as effective eigenmodes of the scheme.

Appendix B

In what follows we relate the problem of optimal efficiency of the memory to the dynamics of excitations number by the time-reversed evolution, and show that the time-reversal approach based on the input signal interaction with "empty" cavity followed by fast excitation transfer to atoms can be considered as the most efficient for a given input signal duration.

Since the incoming, the outgoing and the cavity field together with the collective spin wave form a closed system where total excitation number is conserved, the general solution of the basic evolution equations (23) is represented by a unitary transformation, which one can consider in classical picture. We split the time interval $(0,\mathcal{T})$

to $N \gg 1$ intervals of duration $\epsilon = \mathcal{T}/N$, centered at τ_n, $n = 1 \dots N$, and consider discrete sets of the incoming and the outgoing signal amplitudes: $\tilde{\alpha}^{(in)}(\tau_n) = \sqrt{\epsilon}\alpha^{(in)}(\tau_n)$, and similar for the outgoing field. The transverse mode index is omitted for brevity and will be restored later. The factor $\sqrt{\epsilon}$ allows to evaluate the incoming excitation number at the nth interval as $|\tilde{\alpha}^{(in)}(\tau_n)|^2$. If at the beginning ($\tau = 0$) and at the end ($\tau = \mathcal{T}$) of the write-in cycle one accounts for the non-zero collective spin and the cavity field amplitudes, the $(2+N)$-component column vectors of the form

$$\tilde{\alpha}^{(in)} = \left(\beta(0), \alpha(0), \left\{\sqrt{\epsilon}\alpha^{(in)}(\tau_n)\right\}\right),$$
$$\tilde{\alpha}^{(out)} = \left(\beta(\mathcal{T}), \alpha(\mathcal{T}), \left\{\sqrt{\epsilon}\alpha^{(out)}(\tau_n)\right\}\right), \tag{B.1}$$

represent the essential sets of the initial and final amplitudes.

The unitary amplitudes evolution matrix is introduced via

$$\tilde{\alpha}^{(out)} = \hat{U}\tilde{\alpha}^{(in)}. \tag{B.2}$$

As it follows from the orthogonality and normalization of the rows of $\hat{U}$, the initial vector of amplitudes which allows to excite the collective spin with unit efficiency (that is, gives $\tilde{\alpha}^{(out)} = (1, 0, \{0\})$ is composed by using the row β of $\hat{U}$,

$$\tilde{\alpha}^{(in)} \sim \left(U^*_{\beta\beta}, U^*_{\beta\alpha}, \{U^*_{\beta m}\}\right),$$

where $m = 1 \dots N$. By the write-in we assume that the initial local amplitudes $\beta(0)$, $\alpha(0)$ have zero values, and optimal normalized initial vector of amplitudes which gives maximal $\beta(\mathcal{T})$ and, hence, maximal efficiency, is proportional to the reduced row of $\hat{U}$,

$$\tilde{\alpha}^{(in)} = \frac{1}{\sqrt{1 - (|U_{\beta\beta}|^2 + |U_{\beta\alpha}|^2)}} \left(0, 0, \{U^*_{\beta m}\}\right). \tag{B.3}$$

The collective spin wave amplitude $\beta(\boldsymbol{q})$ and its excitation efficiency by the signal wave $\boldsymbol{q}$ are found by using (B.3) and unit norm of the row β,

$$\eta = |\tilde{\alpha}^{(out)}_\beta|^2 = 1 - \left(|U_{\beta\beta}|^2 + |U_{\beta\alpha}|^2\right). \tag{B.4}$$

We have related in general form the optimal memory efficiency for a given transverse mode of the signal and for a given time shape of the coupling parameter to the values of two elements of the evolution matrix (the Green functions) of the system. Since in our parallel memory the evolution matrix depends on the signal wave transverse momentum, $\hat{U} \to \hat{U}(\boldsymbol{q})$, the optimal input signal shape (B.3) is in general case $\boldsymbol{q}$-dependent (note that in Sect. 4 the input signal optimized for $\boldsymbol{q} = 0$ is considered).

One can rewrite the efficiency (B.4) as:

$$\eta(\boldsymbol{q}) = 1 - \left(\left|U^\dagger_{\beta\beta}(\boldsymbol{q})\right|^2 + \left|U^\dagger_{\alpha\beta}(\boldsymbol{q})\right|^2\right). \tag{B.5}$$

Here the $\hat{U}^\dagger(\boldsymbol{q})$ evolution matrix describes the inverted in time evolution, and the sum in the right side of (B.5) gives, by the definition of the evolution matrix elements, the number of cavity excitations by $\tau = 0$ given the inverted in time evolution started at $\mathcal{T}$ from the specific initial condition, $\tilde{\alpha}^{(out)} = (1, 0, \{0\})$, when the collective spin is excited and other amplitudes are equal to zero,

$$|\beta(\boldsymbol{q}, \mathcal{T})| = 1, \quad \alpha(\boldsymbol{q}, \mathcal{T}) = 0, \quad \left\{\alpha^{(out)}(\boldsymbol{q}, \tau_n)\right\} = 0. \tag{B.6}$$

The inverted in time evolution equations are derived from (23),

$$\frac{\partial \alpha(\boldsymbol{q}, \tau_-)}{\partial \tau_-} = \left[i\tilde{\Delta}(\boldsymbol{q}) - \frac{1}{2}\right]\alpha(\boldsymbol{q}, \tau_-)$$
$$+ i\kappa(\tau_-)\beta(\boldsymbol{q}, \tau_-) + \alpha^{(out)}(0, \boldsymbol{q}, \tau_-),$$
$$\frac{\partial}{\partial \tau_-}\beta(\boldsymbol{q}, \tau_-) = i\kappa(\tau_-)\alpha(\boldsymbol{q}, \tau_-),$$
$$\alpha^{(in)}(0, \boldsymbol{q}, \tau_-) = -\alpha^{(out)}(0, \boldsymbol{q}, \tau_-) + \alpha(\boldsymbol{q}, \tau_-), \tag{B.7}$$

where $\tau_- = \mathcal{T} - \tau$, and the evolution takes place from $\tau_- = 0$ to $\tau_- = \mathcal{T}$. By transforming (B.7) to equations for the excitation numbers we arrive at

$$\frac{d}{d\tau_-}\left(|\beta(\boldsymbol{q}, \tau_-)|^2 + |\alpha(\boldsymbol{q}, \tau_-)|^2\right)$$
$$= -|\alpha(\boldsymbol{q}, \tau_-)|^2 + 2\mathrm{Re}\left[\alpha^*(\boldsymbol{q}, \tau_-)\alpha^{(out)}(0, \boldsymbol{q}, \tau_-)\right]. \tag{B.8}$$

Next, we perform time integral and account for (B.6). This yields for the write-in efficiency

$$\eta(\boldsymbol{q}) = 1 - \left(|\beta(\boldsymbol{q}, \mathcal{T})|^2 + |\alpha(\boldsymbol{q}, \mathcal{T})|^2\right)$$
$$= \int_0^{\mathcal{T}} d\tau_- |\alpha(\boldsymbol{q}, \tau_-)|^2. \tag{B.9}$$

Though this equality does not explicitly depend on $\kappa(\tau)$, it is valid for any time shape of the coupling constant.

Note that equations (B.7) of evolution in time τ_- for the initial condition (B.6) we apply, differ from equations (23) of evolution in physical time τ for the initial condition of the form $\beta(\boldsymbol{q}, \tau = 0) = 1$, $\alpha(\boldsymbol{q}, \tau = 0) = 0$, $\alpha^{(in)}(\boldsymbol{q}, \tau = 0) = 0$, only by inversion of the frequency mismatch and the coupling constant sign.

That is, we can think about the optimization of efficiency (B.9) in terms of equivalent physical evolution, as if τ_- were physical time, with the initially excited collective spin wave, zero initial intracavity field, and zero incoming field amplitude, when interference at the input mirror is eliminated. Since the dimensionless rate of the cavity decay is equal to unity, the right side of (B.9) gives the energy leaking from the cavity by $\tau_- = \mathcal{T}$, and is evidently maximized if one performs at $\tau_- = 0$ fast transfer of excitation from atoms to the intracavity field and then allows for energy to leak from "empty" cavity. In terms of the physical time $\tau = \mathcal{T} - \tau_-$ this is just the optimal mode of memory operation discussed in Section 4.

References

1. K. Hammerer, A.S. Sørensen, E.S. Polzik, Rev. Mod. Phys. **82**, 1041 (2010)
2. C. Simon et al., Eur. Phys. J. D **58**, 1 (2010)
3. A.L. Lvovsky, B.C. Sanders, W. Tittel, Nat. Photon. **3**, 706 (2009)
4. B. Julsgaard, J. Sherson, J. Fiurasek, J.I. Cirac, E.S. Polzik, Nature **432**, 482 (2004)
5. M.P. Hedges, J.J. Longdell, Yongmin Li, M.J. Sellars, Nature **465**, 1052 (2010)
6. M. Hosseini, B.M. Sparkes, G. Campbell, B.C. Buchler, P.K. Lam, Nat. Commun. **2**, 174 (2011)
7. C. Simon, H. de Riedmatten, M. Afzelius, N. Sangouard, H. Zbinden, N. Gisin, Phys. Rev. Lett. **98**, 190503 (2007)
8. D.V. Vasilyev, I.V. Sokolov, E.S. Polzik, Phys. Rev. A **77**, 020302(R) (2008)
9. K. Surmacz, J. Nunn, K. Reim, K.C. Lee, V.O. Lorenz, B. Sussman, I.A. Walmsley, D. Jaksch, Phys. Rev. A **78**, 033806 (2008)
10. D.V. Vasilyev, I.V. Sokolov, E.S. Polzik, Phys. Rev. A **81**, 020302(R) (2010)
11. D.V. Vasilyev, I.V. Sokolov, Eur. Phys. J. D **66**, 294 (2012)
12. T. Golubeva, Yu.M. Golubev, O. Mishina, A. Bramati, J. Laurat, E. Giacobino, Eur. Phys. J. D **66**, 275 (2012)
13. K. Tikhonov, K. Samburskaya, T. Golubeva, Yu. Golubev, Phys. Rev. A **89**, 013811 (2014)
14. E. Zeuthen, A. Grodecka-Grad, A.S. Sørensen, Phys. Rev. A **84**, 043838 (2011)
15. L. Veissier, A. Nicolas, L. Giner, D. Maxein, A. Sheremet, E. Giacobino, J. Laurat, Opt. Lett. **38**, 712 (2013)
16. A. Dantan, A. Bramati, M. Pinard, Phys. Rev. A **71**, 043801 (2005)
17. A.V. Gorshkov, A. Andre, M.D. Lukin, A.S. Sørensen, Phys. Rev. A **76**, 033804 (2007)
18. A. Kalachev, Phys. Rev. A **78**, 043812 (2008)
19. Q.Y. He, M.D. Reid, E. Giacobino, J. Cviklinski, P.D. Drummond, Phys. Rev. A **79**, 022310 (2009)
20. X. Zhang, A. Kalachev, O. Kocharovskaya, Phys. Rev. A **87**, 013811 (2013)
21. M. Afzelius, C. Simon, Phys. Rev. A **82**, 022310 (2010)
22. S.A. Moiseev, S.N. Andrianov, F.F. Gubaidullin, Phys. Rev. A **82**, 022311 (2010)
23. D.S. Goldman, *Information Theory* (Prentice-Hall, New York, 1953)
24. B. Schumacher, M.A. Nielsen, Phys. Rev. A **54**, 2629 (1996)
25. S. Lloyd, Phys. Rev. A **55**, 1613 (1997)
26. A.N. Vetlugin, I.V. Sokolov, Opt. Spectrosc. **115**, 875 (2013)
27. J. Dilley, P. Nisbet, B.W. Shore, A. Kuhn, Phys. Rev. A **85**, 023834 (2012)
28. N.N. Rosanov, *Spatial hysteresis and optical patterns* (Springer, Berlin Heidelberg, New-York, 2002)
29. *Quantum Imaging*, edited by M. Kolobov (Springer Science+Buisiness Media LLC, 2007)
30. A.E. Siegman, *Lasers* (University Science Books, Ca, 1986)